The Abdus Salam International Centre for Theoretical Physics

United Nations Educational, Scientific and Cultural Organization

IAEA International Atomic Energy Agency

2052-51

Summer College on Plasma Physics

10 - 28 August 2009

Alfvén wave filamentation and dispersive phase mixing

Pierre-Louis Sulem

Observatoire de la Côte d'Azur
France

Alfvén wave filamentation and dispersive phase mixing

P.L. Sulem, T. Passot, D. Laveder
CNRS, Observatoire de la Côte d'Azur, Nice

D. Borgogno
BPRG, Dept. of Energetics, Politecnico di Torino

Summer College on Plasma Physics, ICTP, Trieste, August 2009

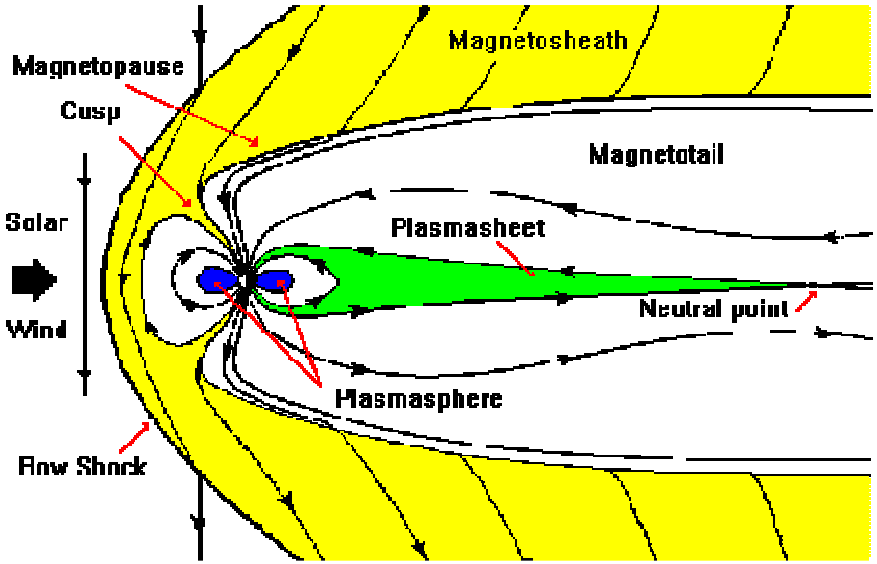

Magnetosheath: transition region between the solar wind and the terrestrial magnetosphere (limited by the bowshock)

Solar wind: flow of collisionless magnetized plasma originating from the expansion of the solar corona. It meets the neighborhood of the earth with a supersonic relative velocity (200 km/s < v < 900 km/s) leading to a shock wave (bow shock).

Quasi-perpendicular shock: when the angle between the interplanetary magnetic field and the normalshock is 45°< θ < 90°.

Quasi-monochromatic dispersive Alfvén waves are commonly observed in the **solar wind** and the **magnetosheath**

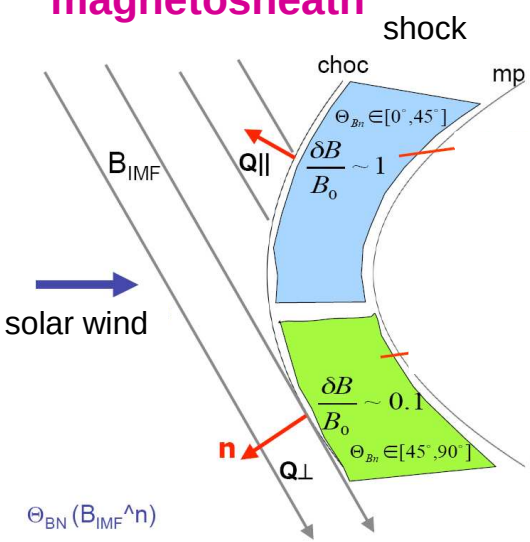

(adapted from Alexandrova's talk)

Observation by CLUSTER satellites downstream the quasi-perpendicular bow shock

(Alexandrova et al., J. Geophys. Res., (2004)

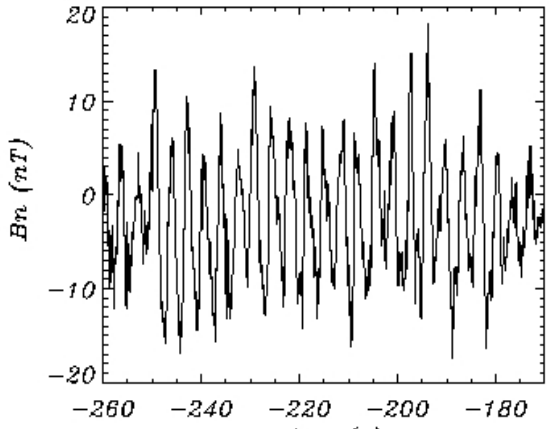

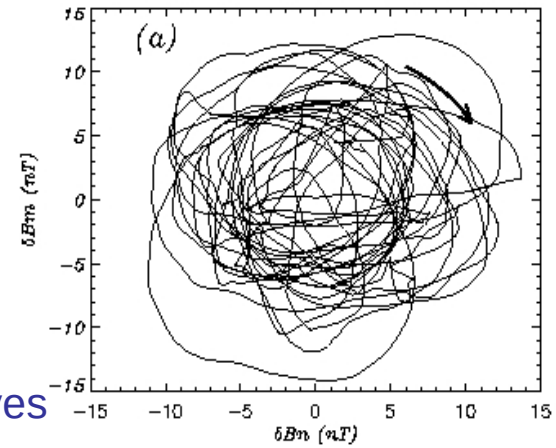

Presence of almost monochromatic left-hand circularly polarized Alfvén waves

Observed magnetic filaments in the magnetosheath behind the quasi perpendicular bow shock (Alexandrova et al., JGR, 2006)

Field aligned magnetic filaments with a radius ~ ion inertial length

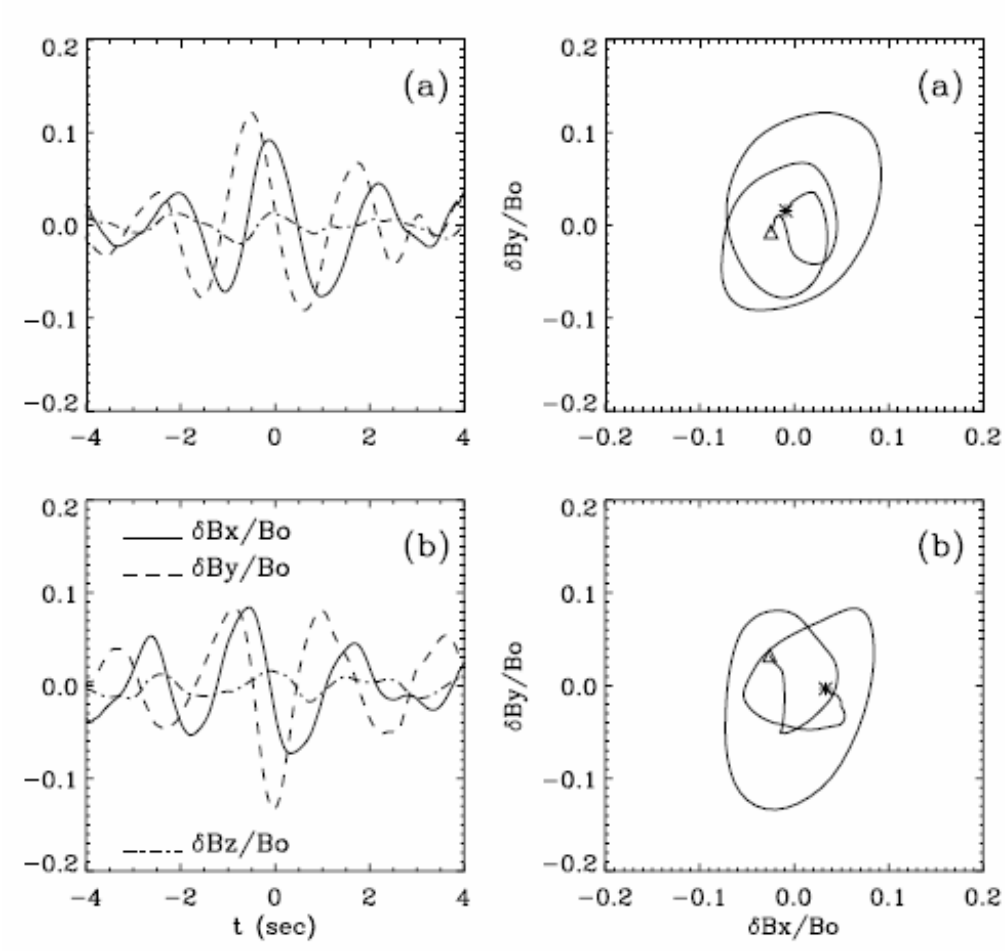

Filamentation instability provides a mechanism to concentrate magnetic energy into filamentary structures (parallel to the ambient field) in conditions where dispersion is significant.

Alternative interpretation: *Alfvén vortices* (exact solutions of the incompressible MHD equations)

Alfvén wave filamentation in an homogeneous plasma was studied in detail in the **Hall-MHD** framework using both asymptotic and numerical approaches.

Hall-MHD equations

$$\partial_t \rho + \nabla.(\rho \mathbf{u}) = 0$$

$$\rho(\partial_t \mathbf{u} + \mathbf{u}.\nabla \mathbf{u}) = -\frac{\beta}{\gamma}\nabla \rho^\gamma + (\nabla \times \mathbf{b}) \times \mathbf{b}$$

$$\partial_t \mathbf{b} - \nabla \times (\mathbf{u} \times \mathbf{b}) = -\frac{1}{R_i}\nabla \times (\frac{1}{\rho}(\nabla \times \mathbf{b}) \times \mathbf{b})$$

$$\nabla.\mathbf{b} = 0$$

Hall term: **dispersive** effects

velocity unit: Alfvén speed
length unit : $R_i \times$ ion inertial length
time unit: $R_i \times$ ion gyroperiod
density unit: mean density
magnetic field unit: ambient field

Hall-MHD: Bi-fluid description where electron inertia is neglected

1) For large-scale transverse perturbations of a ***small-amplitude*** parallel Alfvén wave, modulation analysis leads to the 2D NLS equation:

$$i\partial_t B + \alpha \Delta_\perp B - k v_g \left(\frac{1}{v_g^2} - \frac{k^4}{4(\beta+1)\omega^4} \right) |B|^2 B = 0,$$

$$v_g = \omega' = \frac{2\omega^3}{k(k^2+\omega^2)} \qquad \alpha = \left(\frac{k\omega}{k^2+\omega^2} \right) \left(\frac{\omega^2}{2k^3} - \frac{\beta k}{2(\beta k^2 - \omega^2)} \right)$$

B : wave amplitude

k : wave number

ω : wave frequency

Instability when the diffraction and nonlinear coupling coefficients have the ***same sign***

(typically **β>1**, when the pump wavelength is large compared with the ion inertial length)

NLS equation: filamentation instability leads to wave collapse (finite-time singularity).

Physically: formation of intense magnetic filaments.

Shukla & Stenflo, Astrophys., Space Sci. 1989
Champeaux, Passot & Sulem, JPP 1997

2) Direct numerical simulations of 3D Hall-MHD

(Laveder, Passot & Sulem, PoP 2002)

Small amplitude wave: (NLS regime):
Large-scale instability
Intense amplification

β=1.5

$|B_\perp|$

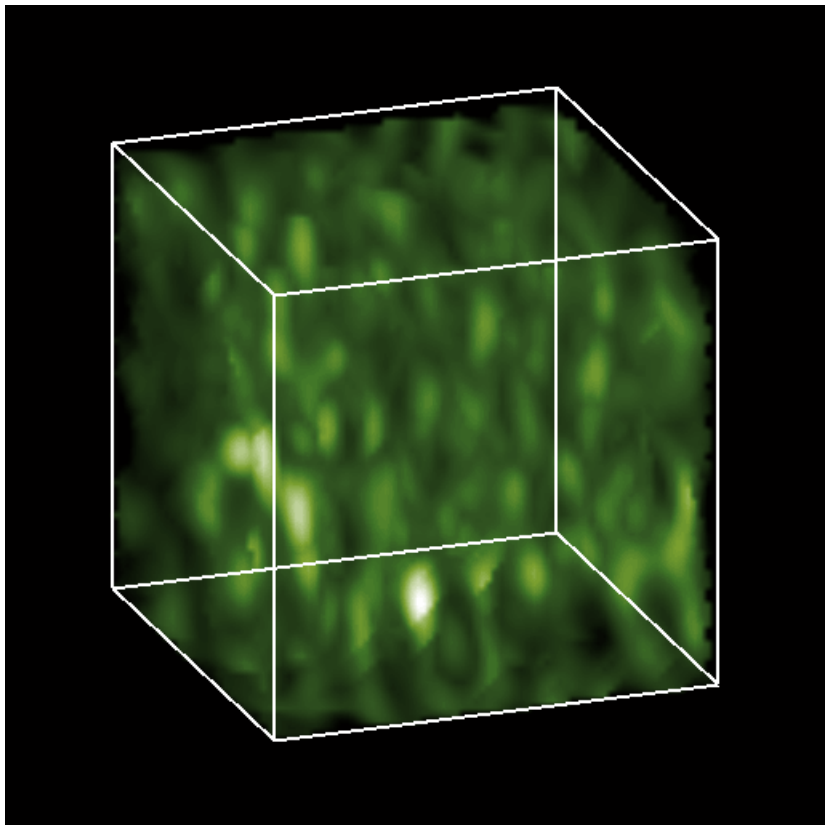

2) Direct numerical simulations of 3D Hall-MHD *(Laveder, Passot & Sulem, PoP 2002a,b)*

β=1.5

Small amplitude wave: (NLS regime)
Large-scale instability
Intense amplification

$|B_\perp|$

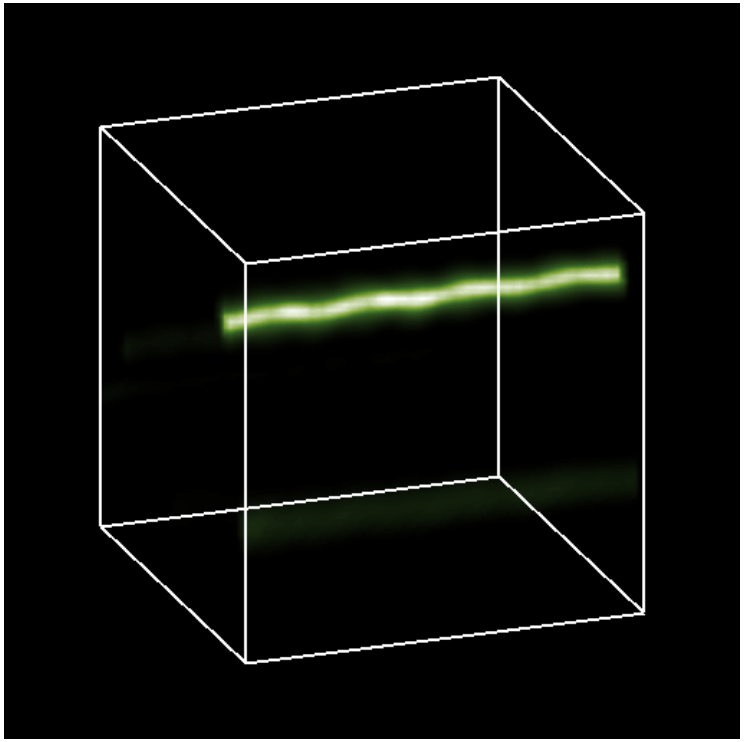

Large amplitude wave:
small-scale instability
Curled filaments
Moderate amplification

$|B_\perp|$

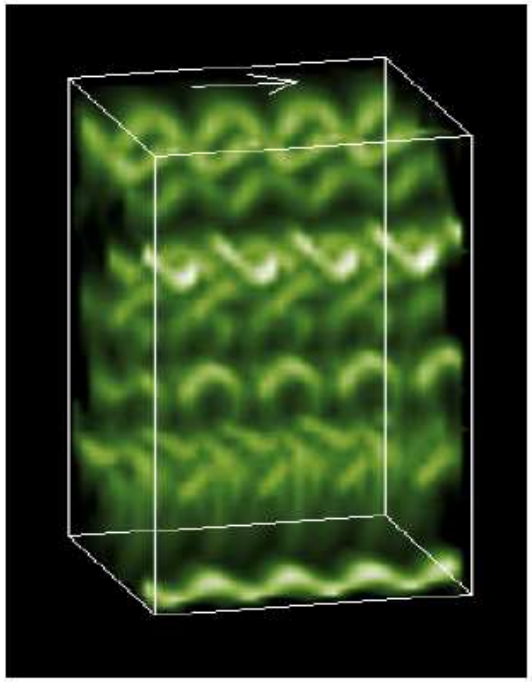

Effect of plasma inhomogeneities on Alfvén wave filamentation

Inhomogeneities: density channels (ducts) aligned with the ambient magnetic field. The plasma density inside a duct can be *higher* (high-density duct) or *lower* (low-density duct) than the density outside the duct.

Field-aligned density channels:

- are frequently encountered in the magnetosphere where they play the role of ducts that guide whistler waves (Karpman and Kaufman 1982, Pasmanik and Trakhtengerts 2005, Stretlsov et al. 2006, 2007)

- density cavities are encountered in auroral acceleration regions where they affect the interaction of Alfvén waves with the plasma, with consequences on the electron acceleration (Génot, Louarn and Mottez 2004)

- can also correspond to pressure balanced structures almost aligned with the ambient field, resulting from mirror instabilities.

Hall-MHD simulations in the presence of a density channel

$\beta = 1.5$

Low-density channel of 10% magnitude (relatively to equilibrium state)

Filamentation faster but early arrested

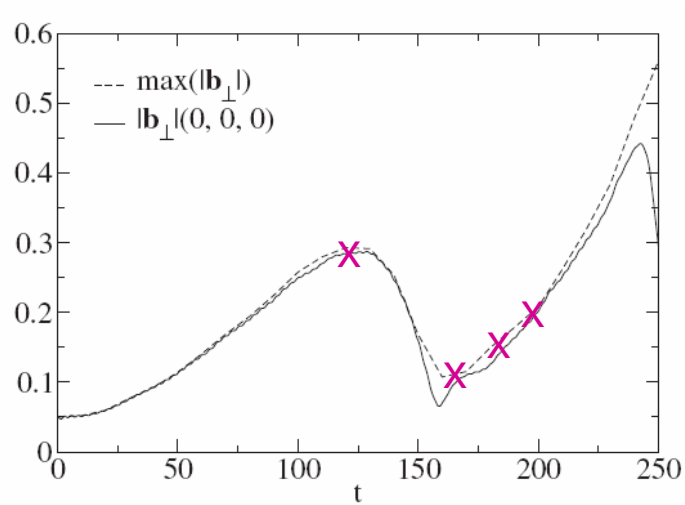

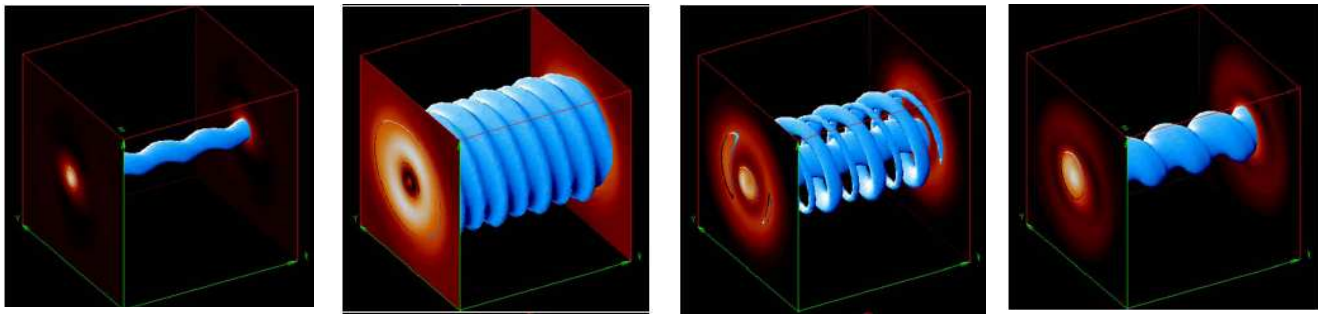

t = 120 t=160 t=180 t=200

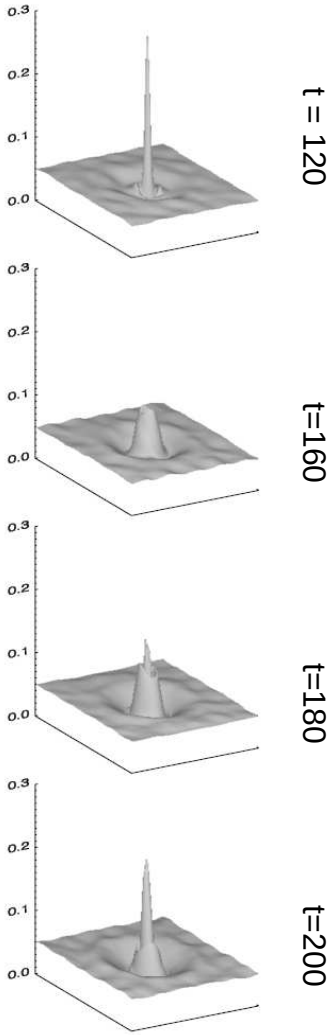

Amplitude in the transverse plane x=0

At the level of NLS eq. the density channel acts as an attracting linear potential

Hall-MHD simulation

Longitudinally averaged intensity

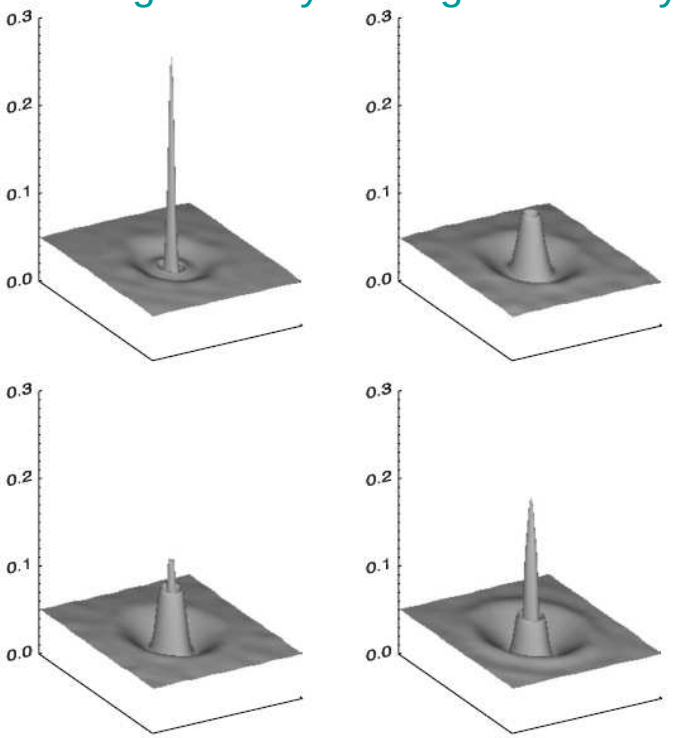

NLS with linear potential

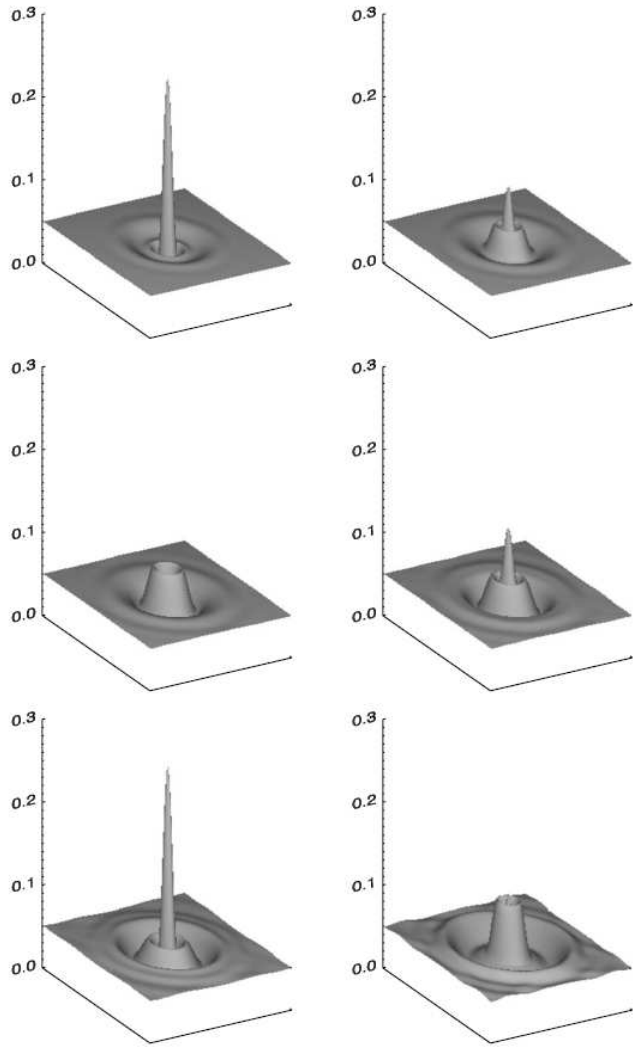

Arrest of collapse by attracting potential at critical dimension:
Linear potential isolates a small fraction of the wave energy, insufficient to focus, while the rest of the energy disperses, then making nonlinear effects not strong enough to produce blowup. This can lead to an oscillatory beam.

$$i\partial_t B + \alpha\Delta_\perp B + \boxed{\frac{kv_g}{2}\left(1+\frac{\beta}{1+\beta}\frac{k^2}{\omega^2}\right)\rho_c B} - kv_g\left(\frac{1}{v_g^2} - \frac{k^4}{4(\beta+1)\omega^4}\right)|B|^2 B = 0$$

linear potential

$$\rho_c = -h\exp[-(y^2+z^2)/d^2]$$

(initial density perturbation)

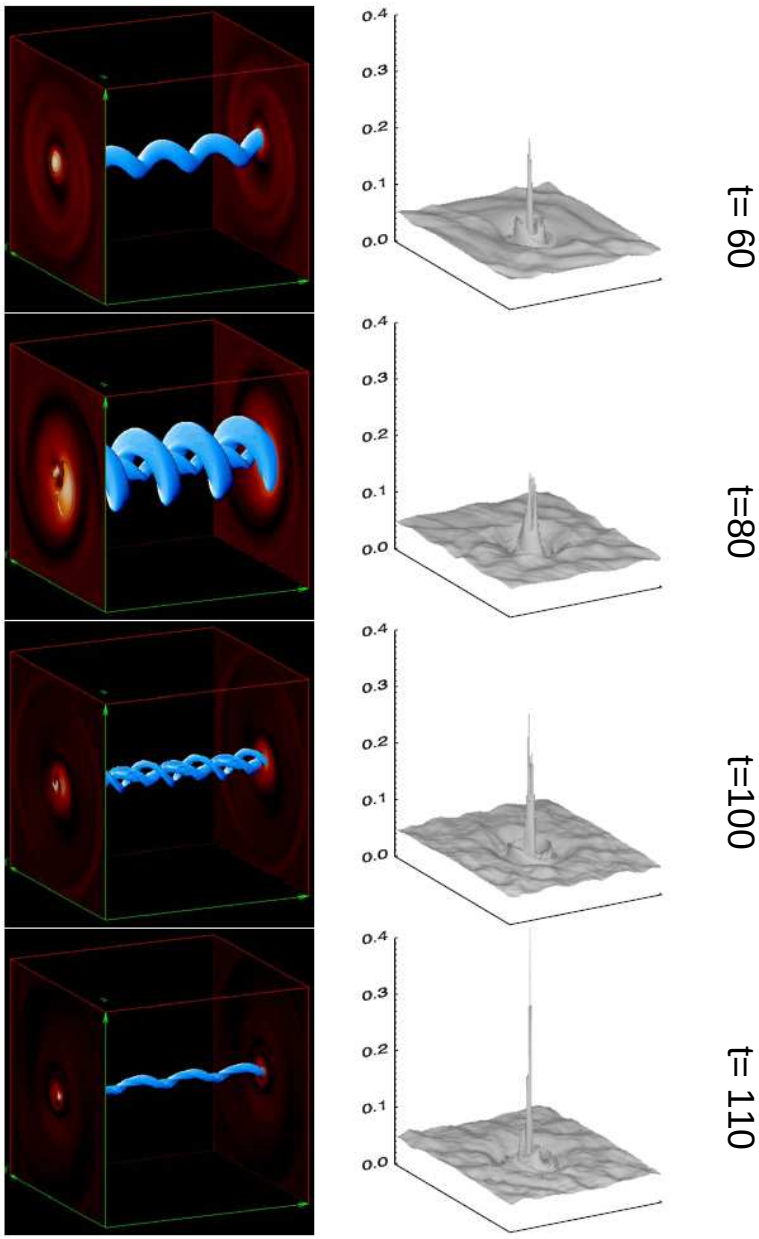

$\beta = 1.5$

Low-density channel
of 30% magnitude

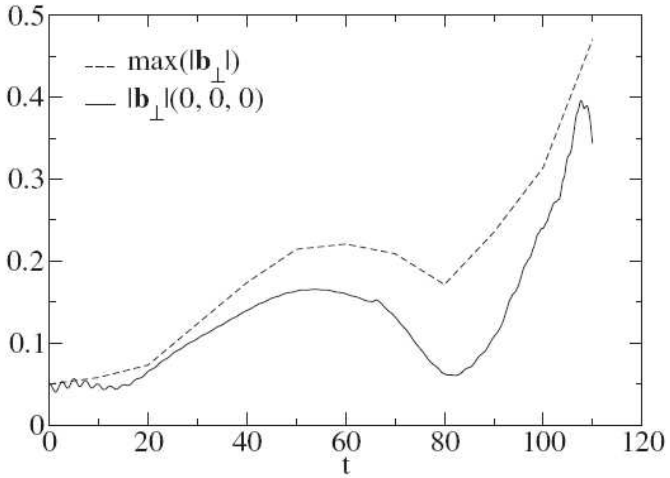

The early time filament is no longer straight
but curled (characterized by the pump wavelength)

β=1.5 and high-density channel (repulsing linear potential), magnetic field is expulsed, leading to a magnetic hole.

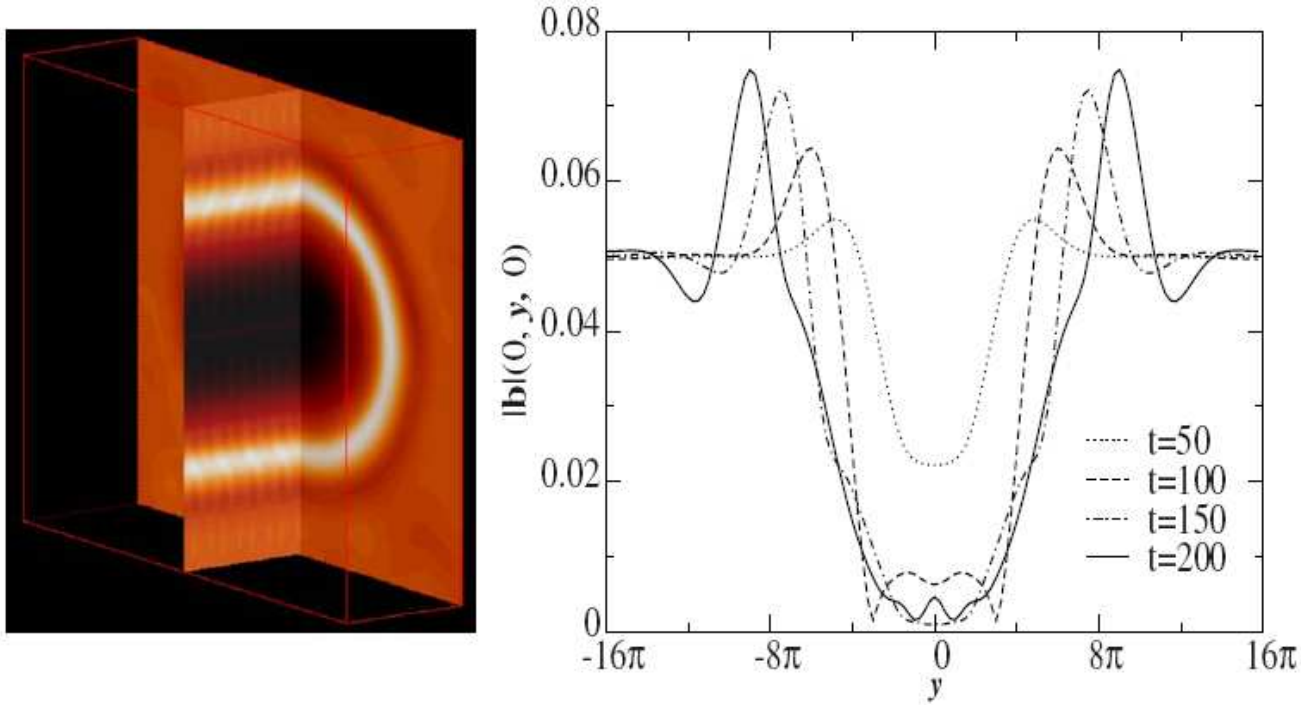

FIG. 8. (Color online) Left: Longitudinal and (whole) transverse sections of the pipe structure associated with the wave amplitude at time $t=200$, from a HMHD simulation with $\beta=1.5$ and an initial density hump of amplitude 0.1. Right: profile of the wave amplitude at times $t=50$, 100, 150, 200, 40, along the line $x=z=0$.

Filamentation at **low β**, in a **high-density** channel (20%)

The density channel provides a lens effect.

β=0.3

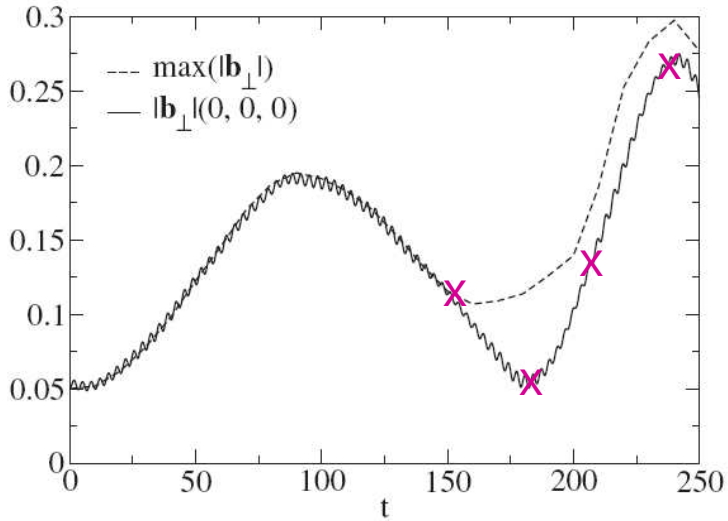

t=150

t=180

t=210

t=230

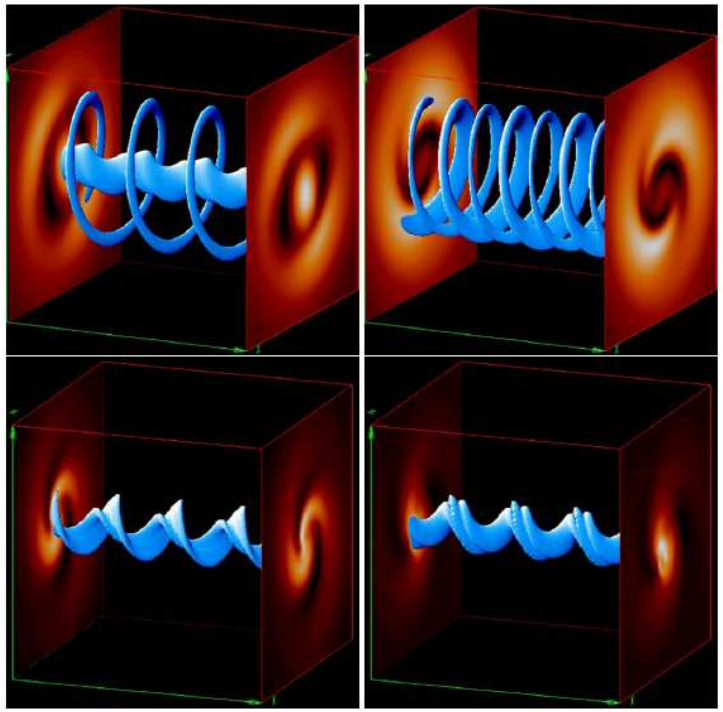

NLS simulation

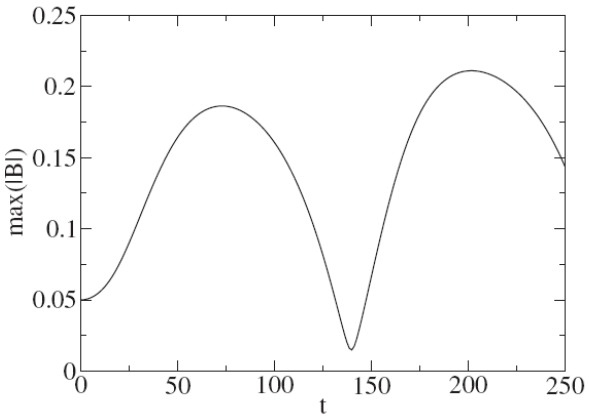

Influence of the decay instability

β= 0.05
High-density channel (10%)

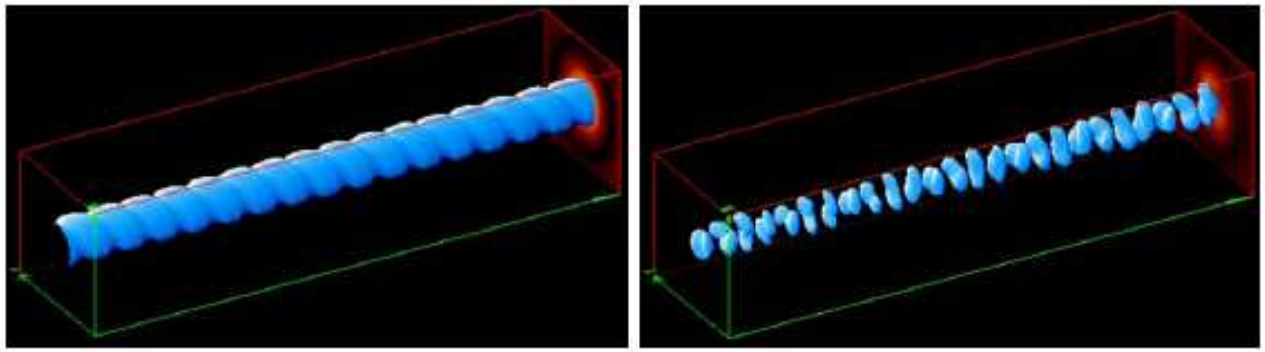

t=230 t=290

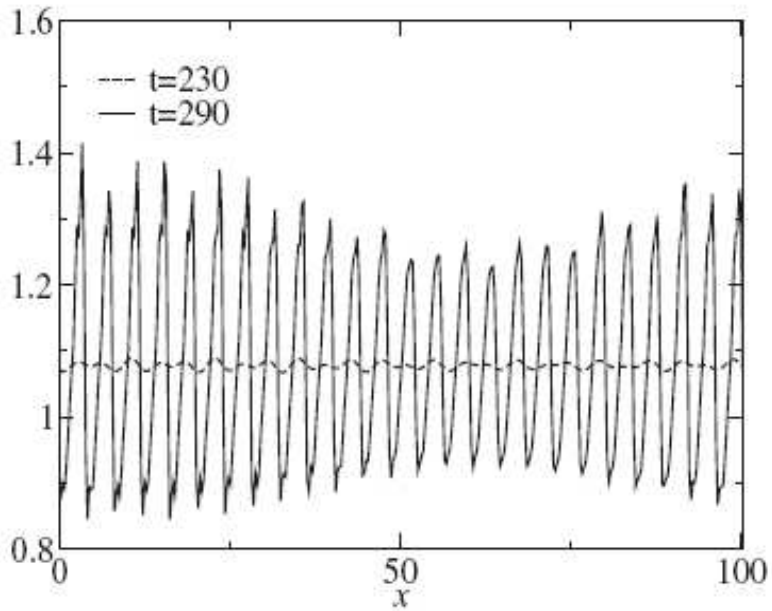

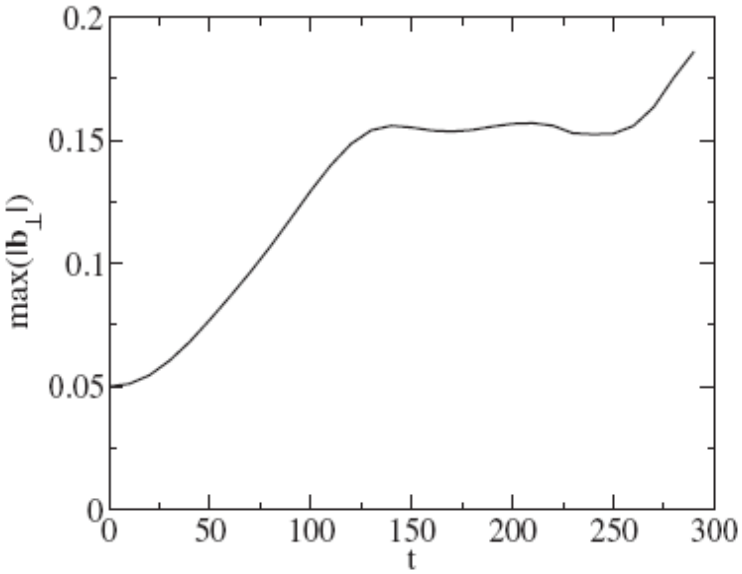

Extension to random arrays of density channels

β = 1.5; low-density channel

β = 0.3; high density channel

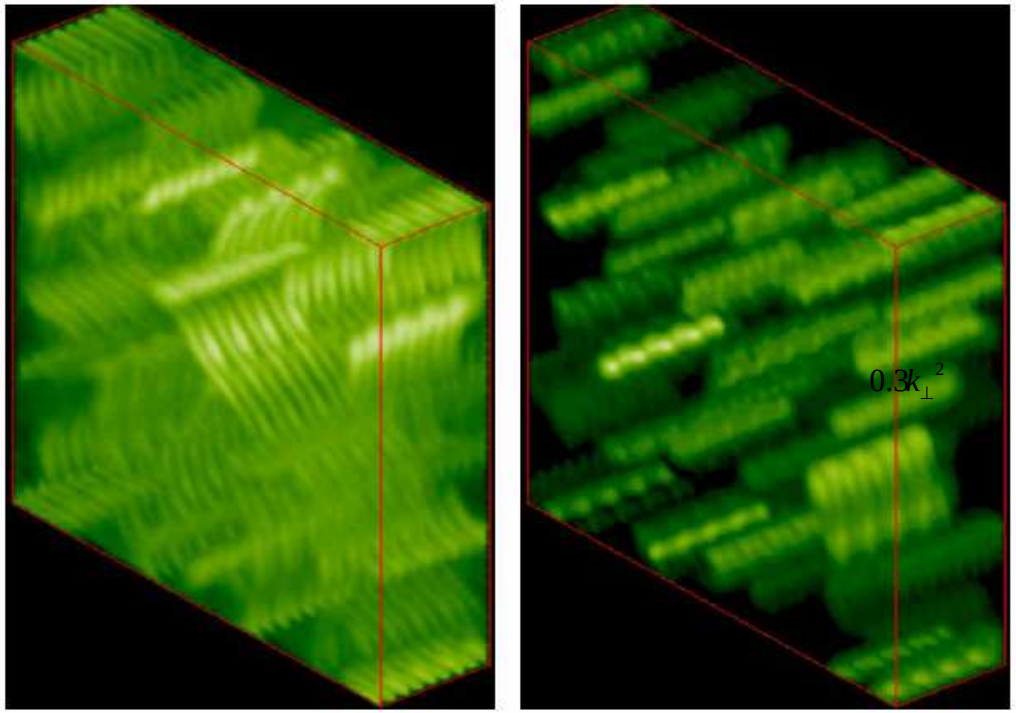

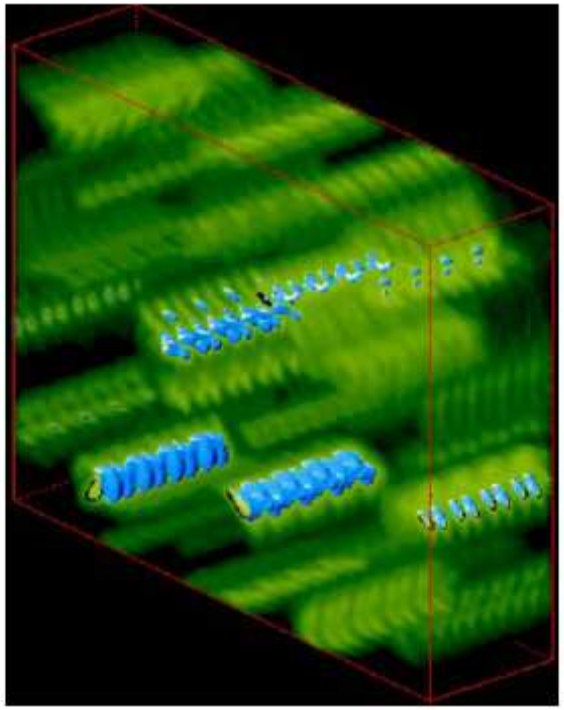

Gaussian random initial perturbation with a spectrum

$$0.3k_\perp^2 \exp\{-(k_\perp/8)^2\}$$

The dispersionless regime

$\beta = 1.5$

Low-density channel (10%)

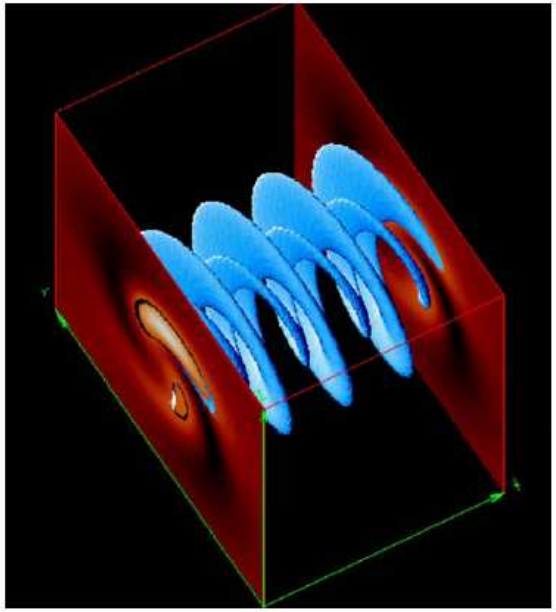

wave amplitude

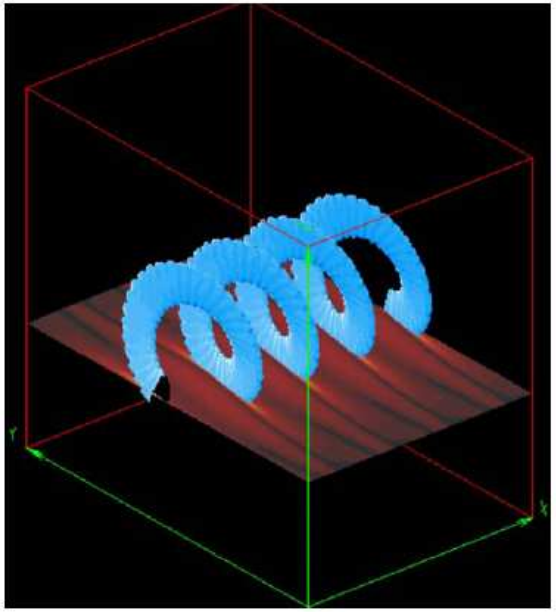

density gradient

No magnetic filaments
but magnetic sheets

Formation of sharp longitudinal gradients (oblique shocks).
Integration is to be interrupted at ealy times (t=40).

Non-dispersive Alfvén waves in an inhomogeneous medium, subject to viscous and Ohmic dissipations are often considered to address the phenomenon of **phase-mixing**, in modeling **solar corona heating**
(Heyvert & Priest 1983, Ireland & Priest 1997).

Alfvén-wave phase mixing

AW are difficult to dissipate.
A possibility to enhance AW dissipation is through small-scale formation.

Phase mixing occurs when a linearly polarized AW propagates in the plasma with transverse density inhomogeneity (large-amplitude high-density channel).

An initially plane AW front is then progressively distorted, because of different Alfvén speeds across the field.

This creates stronger gradients across the field (in the inhomogeneous regions).

In the case of finite resistivity, dissipation is thus greatly enhanced.

Phase mixing is believed to provide substantial **plasma heating.**
(application of the heating of open magnetic structures in the solar corona)

As transverse smaller and smaller scales are formed, MHD approximation is violated. ***Kinetic effects become relevant***.

Particle in cell simulations performed in **2D** (with reduced mass ratio)
(retain kinetic ion and electron scales) *(Tsilkauri et al. 2005, Mottez et al. 2006)*

Influence of (ion) kinetic effect in 3D: a **Landau-fluid** description

(Borgogno et al., NPG 2009)

- Extension of anisotropic Hall MHD by retaining **Landau damping and FLR corrections**: closure of the fluid hierarchy in a way consistent with the low-frequency linear kinetic theory

(Snyder, Hammet & Dorland PoP 1997; Passot & Sulem, PoP 2003, 2005, 2007)

- Ion equations *(electron inertia neglected)*

Electrons are viewed as an (isothermal) fluid with a scalar pressure
(retaining electron Landau damping possible).

$$\frac{\partial \rho}{\partial t} + \boldsymbol{\nabla} \cdot (\rho \mathbf{u}_p) = 0$$

$$\frac{\partial \mathbf{u}_p}{\partial t} + \mathbf{u}_p \cdot \boldsymbol{\nabla} \mathbf{u}_p + \frac{\beta_p}{2\rho} \boldsymbol{\nabla} \cdot (p_{\perp p} \mathbf{n} + p_{\| p} \boldsymbol{\tau} + \boldsymbol{\Pi} + p_e \mathbf{I}) - \frac{1}{\rho} \left[(\mathbf{b} \cdot \boldsymbol{\nabla}) \mathbf{b} - \frac{1}{2} \boldsymbol{\nabla} |\mathbf{b}|^2 \right] = 0$$

$$\frac{\partial \mathbf{b}}{\partial t} = \boldsymbol{\nabla} \times (\mathbf{u}_p \times \mathbf{b}) - \frac{1}{R} \boldsymbol{\nabla} \times \left[\frac{(\boldsymbol{\nabla} \times \mathbf{b}) \times \mathbf{b}}{\rho} \right]$$

$$\frac{\partial p_\perp}{\partial t} + \nabla \cdot (p_\perp \mathbf{u}) + p_\perp \boldsymbol{\nabla} \cdot \mathbf{u} - p_\perp \mathbf{b} \cdot \boldsymbol{\nabla} \mathbf{u} \cdot \mathbf{b} + \boldsymbol{\nabla} \cdot (q_\perp \mathbf{b}) + q_\perp \boldsymbol{\nabla} \cdot \mathbf{b} = 0$$

$$\frac{\partial p_\|}{\partial t} + \nabla \cdot (\mathbf{u} p_\|) + 2 p_\| \mathbf{b} \cdot \boldsymbol{\nabla} \mathbf{u} \cdot \mathbf{b} + \boldsymbol{\nabla} \cdot (q_\| \mathbf{b}) - 2 q_\perp \boldsymbol{\nabla} \cdot \mathbf{b} = 0$$

(non gyrotropic heat flux contributions neglected)

where $\mathbf{n} = \mathbf{I} - \widehat{\mathbf{b}} \otimes \widehat{\mathbf{b}}\,, \quad \boldsymbol{\tau} = \widehat{\mathbf{b}} \otimes \widehat{\mathbf{b}}\,, \quad \widehat{\mathbf{b}} = \mathbf{B}/B\,, \quad R = L/l_i, \quad \beta = 8\pi p_{\|p}^{(0)}/B_0^2$

The Landau-fluid closure

In the framework of the *linear kinetic theory* taken *in the low-frequency (here also in the long-wavelength) limit*, the various moments are expressed in terms of the electromagnetic fluctuations.

These expressions involve the phase velocity through the plasma response (or the plasma dispersion) function (a quantity not suitable for initial value problems).

The closure consists in eliminating the plasma response function as often as possible by substitutions in terms of the lower moments.

In the few terms where it cannot be eliminated, the plasma response function is replaced by Padé approximants of suitable order, which introduces a Hilbert transform, physically associated with (ion) Landau damping.

- Third order momentum closure

Hilbert transform (signature of Landau damping)

$$\left(\frac{d}{dt}+\frac{\sqrt{\pi\beta_p}}{4(1-\frac{3\pi}{8})}\mathcal{H}\partial_z\right)q_{\|}=\frac{1}{1-\frac{3\pi}{8}}\frac{\beta_p}{2}\partial_z(p_{\|}-\rho)$$

$$\mathcal{H}f(z)=\frac{1}{\pi}VP\int_{-\infty}^{+\infty}\frac{f(z')}{z-z'}dz'$$

$$\left(\frac{d}{dt}-\frac{\sqrt{\pi\beta_p}}{2}\mathcal{H}\partial_z\right)q_{\perp}=\frac{\beta_p}{2}\frac{T_{\perp p}^{(0)}}{T_{\|p}^{(0)}}\partial_z\left[\left(1-\frac{T_{\perp p}^{(0)}}{T_{\|p}^{(0)}}\right)|b|-\left(\frac{T_{\|p}^{(0)}}{T_{\perp p}^{(0)}}p_{\perp}-\rho\right)\right]$$

- Ion gyroviscous tensor

$$\Pi_{xx}=-\Pi_{yy}=-\frac{p_{\perp}}{2R}(\partial_y u_x+\partial_x u_y)\,,$$

$$\Pi_{xy}=\Pi_{yx}=-\frac{p_{\perp}}{2R}(\partial_y u_y-\partial_x u_x)$$

$$\Pi_{yz}=\Pi_{zy}=\frac{1}{R}[2p_{\|}\partial_z u_x+p_{\perp}(\partial_x u_z-\partial_z u_x)]$$

$$\Pi_{xz}=\Pi_{zx}=-\frac{1}{R}[2p_{\|}\partial_z u_y+p_{\perp}(\partial_y u_z-\partial_z u_y)]\,,\qquad \Pi_{zz}=0$$

Closure possible at a higher order: for example, retain the nonlinear equations for the gyrotropic heat fluxes and write a closure equations for the gyrotropic components of the 4th order moments. Nongyrotropic components of the heat fluxes and fourth order moments can also be modelized (Goswami et al. 05, Passot & Sulem 07).

In a homogeneous medium, filamentation (that requires $\beta>1$) is strongly inhibited by ion Landau damping.

Special interest of dealing with filamentation in the presence of a density channel in a collisionless plasma
(permits in some instances small scale formation at small β).

Filamentation in a high-density channel of moderate amplitude (10%)

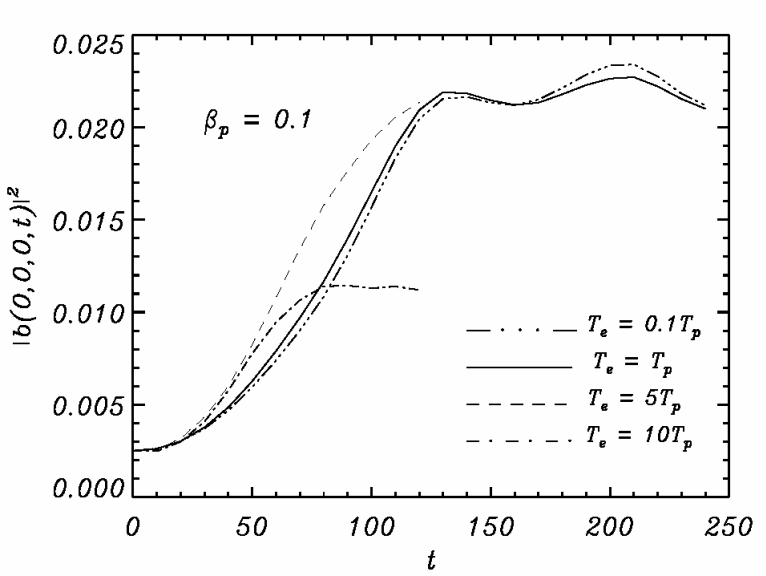

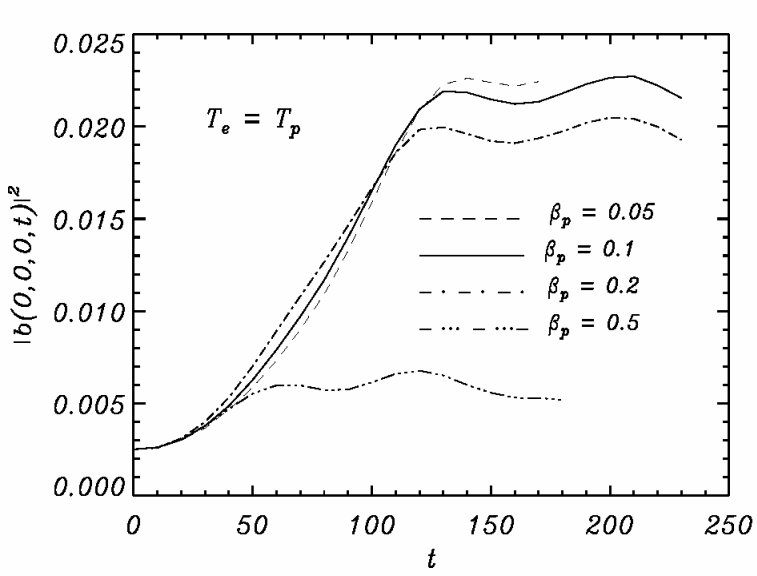

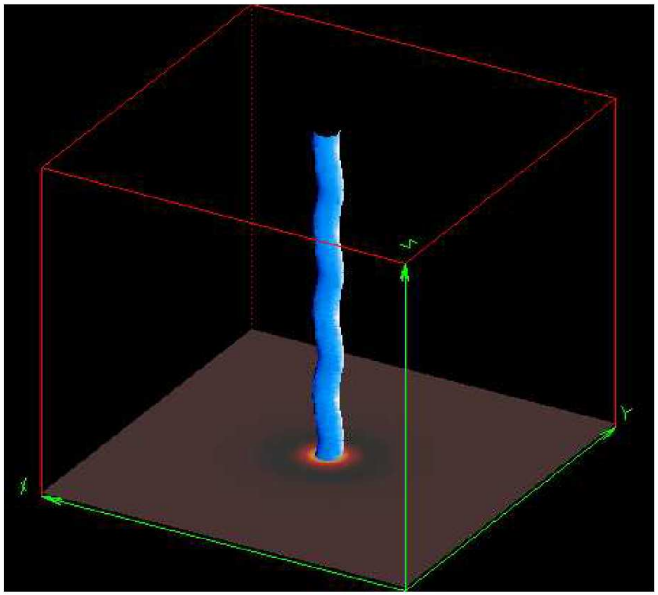

- Wave intensity amplification: ~ factor 10
- Evolution to quasi-stationary with slow oscillations
- Transverse scale prescribed ~ density channel width

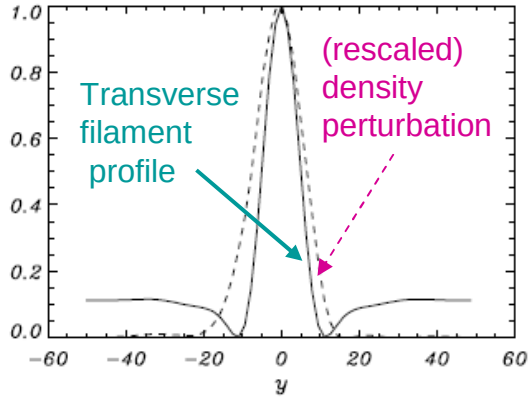

$t=220$

$T_e=T_p$

$\beta_p=0.1$

Comparison between Landau fluid and hybrid PIC simulations

(Borgogno et al. NPG2008)

$$T_e / T_p = 1/30$$
$$\beta_p = 0.3 \quad \beta_e = 0.01$$

Landau fluid | PIC

Instants of maximal amplitude / minimal amplitude on the central axis

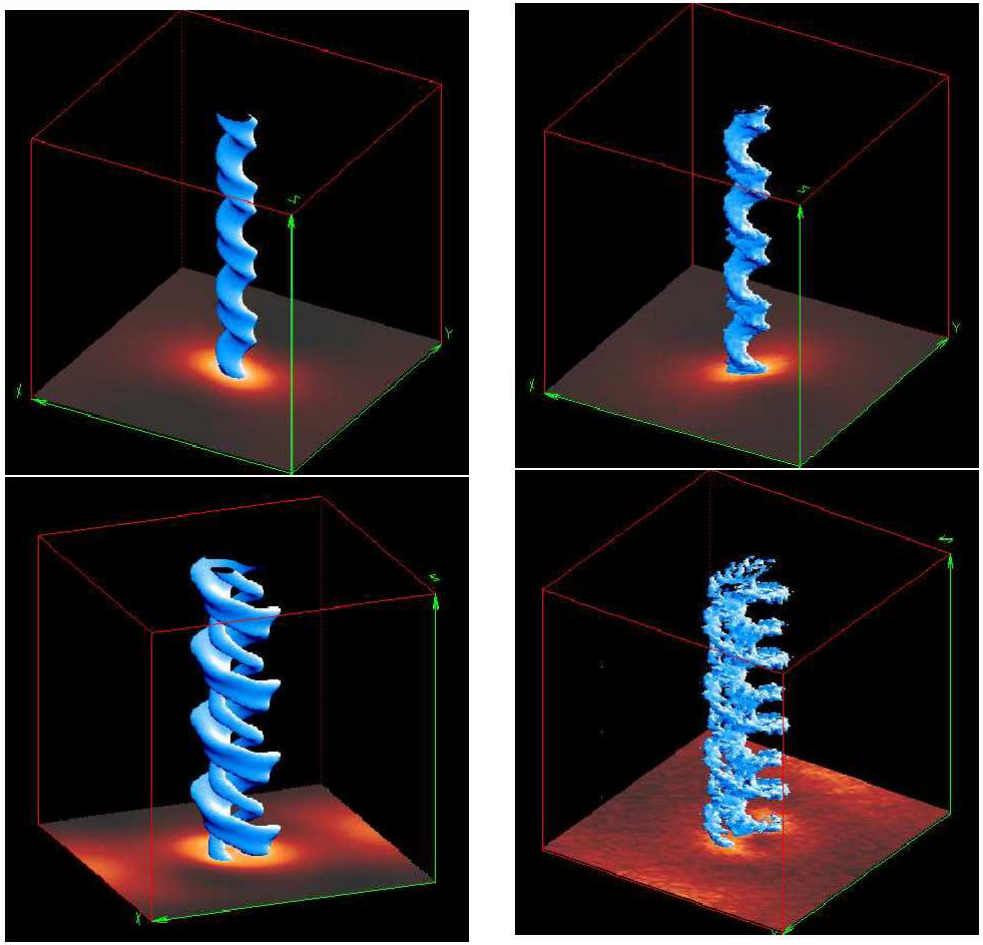

Moderate amplification of the wave intensity.

Slow oscillations of the maximum amplitude

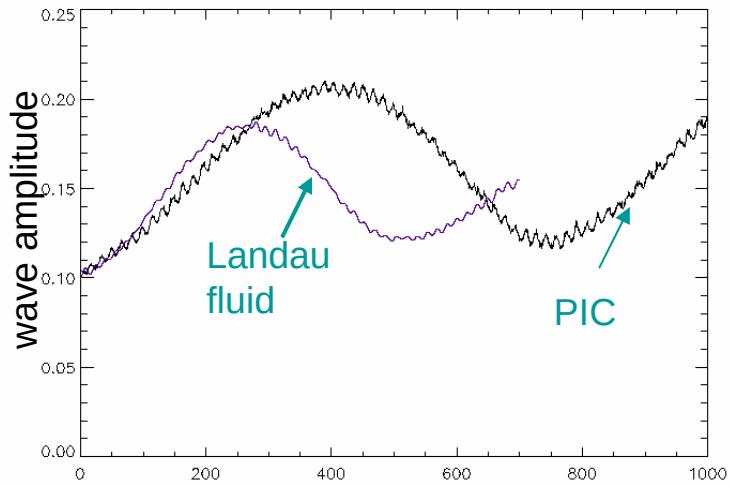

Wave amplitude on the central axis

Qualitative agreement. Possible sources of discrepency:
Nonlinear kinetic effects not retained by Landau fluid
Delicate initialization of the PIC simulation

Alfvén wave dynamics in presence of a stronger (50%) density enhancement leads to dispersive phase mixing

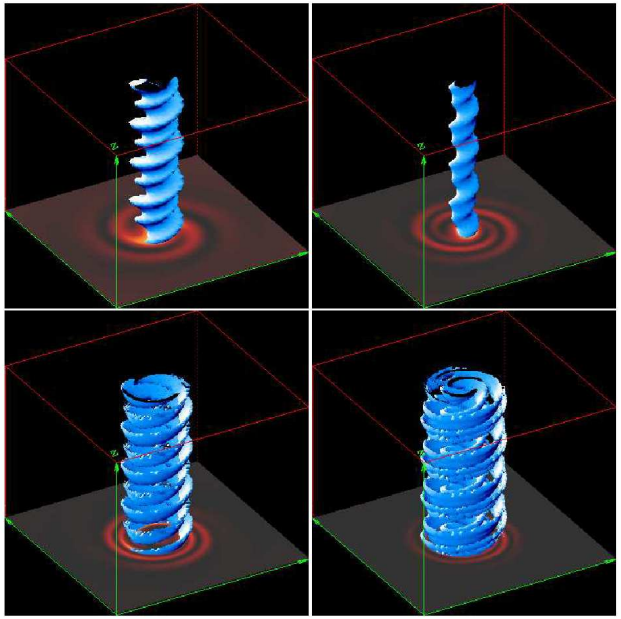

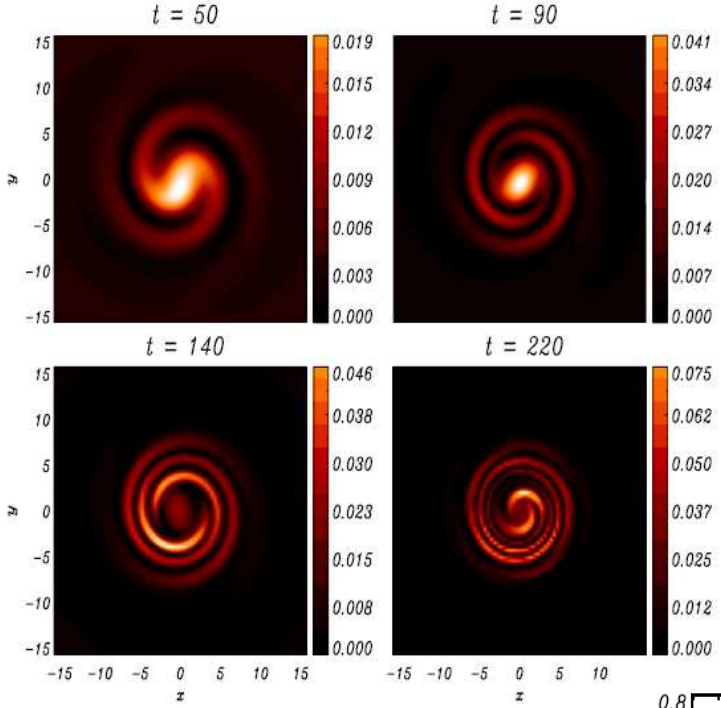

Early formation of magnetic filament is followed by onset of helical ribbons and development of strong gradients

Magnetic structures at different times and corresponding wave-amplitude color plots in a transverse plane

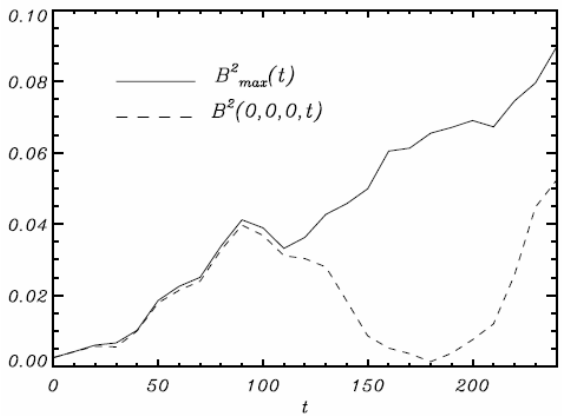

Generation of transverse scales smaller than ion Larmor radius.

Dispersive phase mixing

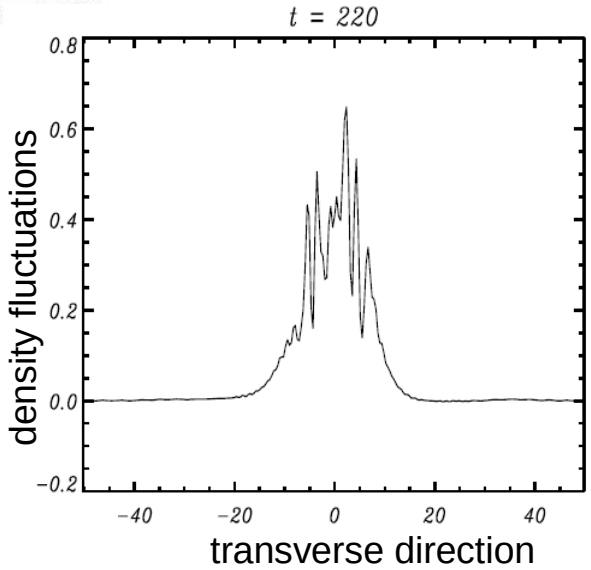

Larger initial density perturbation (100%)

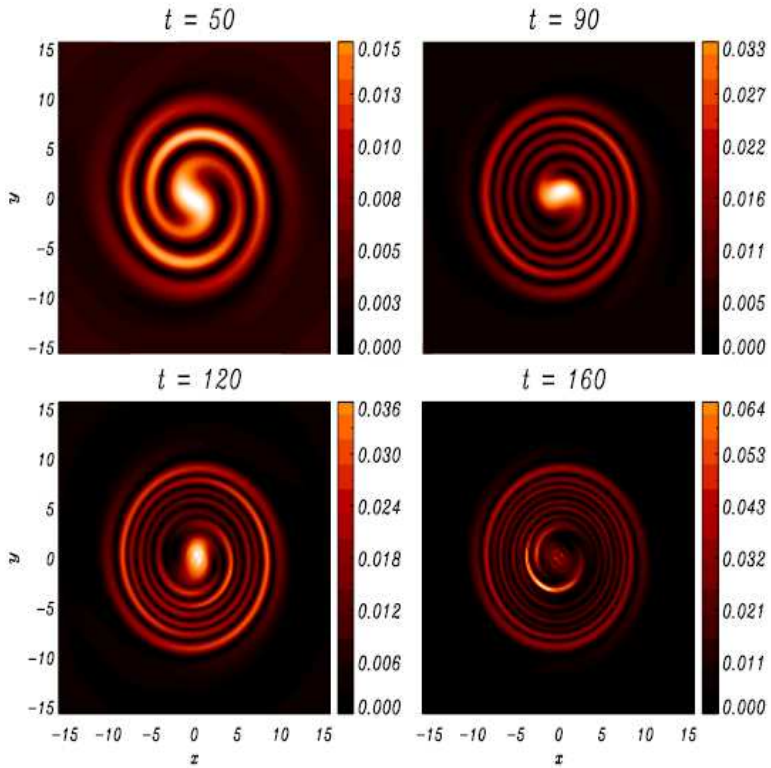

Development of **strong gradients**

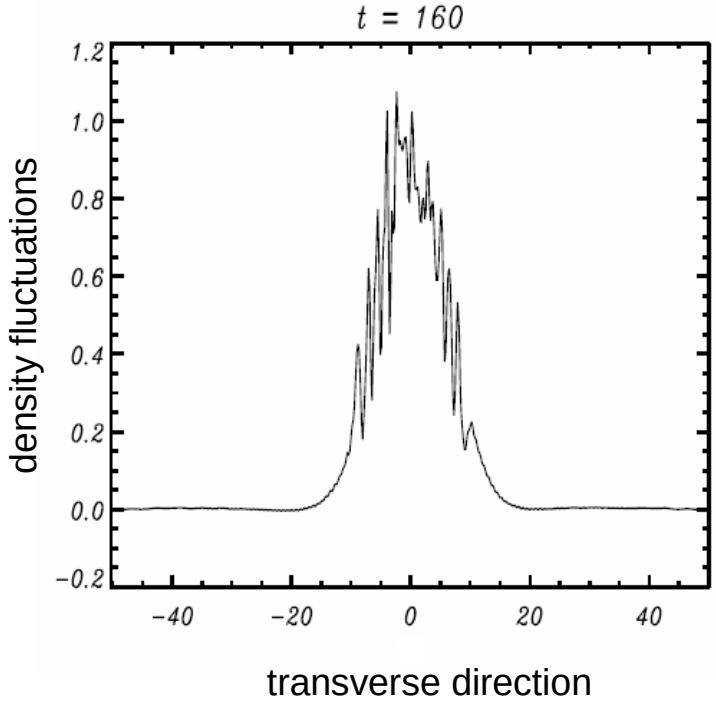

Generation of **transverse scales smaller than ion Larmor radius**.

Similar structures are visible on the perpendicular and parallel temperature fluctuations. The mean temperatures are nevertheless not affected, (consistent with the purely longitudinal effect of the Landau damping that does not dissipate transverse fluctuations).

Conclusions

Density channel parallel to the ambient magnetic field permits
Alfvén wave filamentation in a low-beta plasma (density-induced lensing effect).

In the case of a high-density channel of large enough amplitude:

early formation of a magnetic filament with moderate intensity
and a size prescribed by the channel

followed by the onset of more intense ribbon-like magnetic structures
whose transverse scale decreases as the initial density enhancement is increased,
and can easily be smaller than the ion Larmor radius.

Contrast with usual phase mixing in nondispersive MHD where strong gradients are concentrated on rather localized oblique shocks.

2D PIC simulations *(Tsiklauri et al.05, Mottez et al.06)* with density enhancement of a few hundreds of per cent, lead to the development of fluctuations at scales of the order of the electron Larmor radius: this permits electron acceleration.

Importance of 3D geometry: formation of **strong gradients**
on extended spatial regions with the shape of **thin helical ribbons.**

Work in progress: Add weak collisions and estimate dissipation as the pump wavenumber (and thus the wave dispersion) is varied.